

Title: **AN ASSESSMENT OF THE VALIDITY OF
CERIUM OXIDE AS A SURROGATE FOR
PLUTONIUM OXIDE GALLIUM REMOVAL
STUDIES**

Author(s): David G. Kolman
YoungSoo Park
Marius Stan
Robert J. Hanrahan Jr.
Darryl P. Butt

Submitted to:

<http://lib-www.lanl.gov/la-pubs/00326555.pdf>



Los Alamos
NATIONAL LABORATORY

Los Alamos National Laboratory, an affirmative action/equal opportunity employer, is operated by the University of California for the U.S. Department of Energy under contract W-7405-ENG-36. By acceptance of this article, the publisher recognizes that the U.S. Government retains a nonexclusive, royalty-free license to publish or reproduce the published form of this contribution, or to allow others to do so, for U.S. Government purposes. The Los Alamos National Laboratory requests that the publisher identify this article as work performed under the auspices of the U.S. Department of Energy. Los Alamos National Laboratory strongly supports academic freedom and a researcher's right to publish; therefore, the Laboratory as an institution does not endorse the viewpoint of a publication or guarantee its technical correctness.

AN ASSESSMENT OF THE VALIDITY OF CERIUM OXIDE AS A SURROGATE FOR PLUTONIUM OXIDE GALLIUM REMOVAL STUDIES

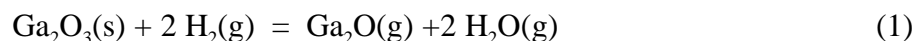
David G. Kolman, YoungSoo Park, Marius Stan, Robert J. Hanrahan Jr., and Darryl P. Butt

Background

A 1996 Record of Decision announced that the United States would pursue a dual-track strategy for the disposition of surplus weapons-grade plutonium. One disposition method involves the conversion of weapons-grade plutonium to mixed oxide (MOX) fuel. However, weapons grade plutonium contains approximately 1% gallium. Gallium is known to degrade the properties of many metallic materials via corrosion, embrittlement, or intermetallic compound formation. Thus, gallium-induced fuel rod cladding failure was identified as a possible concern early in this program. This possibility was investigated by Oak Ridge National Laboratory. Other concerns which have arisen include the effects of gallium on the microstructure and sinterability of the fuel and the consequent effects on fuel performance. Moreover there are concerns that the material output following pit disassembly and conversion will be classified due to a linkage between gallium concentration and pit type. It is therefore desirable to remove the gallium from the weapons-grade plutonium oxide to a sufficiently low level.

Methods for purifying plutonium metal have long been established. These methods use acid solutions to dissolve and concentrate the metal. However, these methods can produce significant mixed waste, that is, waste containing both radioactive and chemical hazards. The volume of waste produced from the aqueous purification of thousands of weapons would be expensive to treat and dispose. Therefore, a "dry" method of purification is highly desirable.

Recently, a dry gallium removal research program commenced. Based on initial calculations, it appeared that a particular form of gallium (gallium suboxide, Ga_2O) could be evaporated from plutonium oxide in the presence of a reducing agent, such as small amounts of hydrogen dry gas within an inert environment:¹



Initial tests using ceria-based material (as a surrogate for PuO_2) showed that thermally-induced gallium removal (TIGR) from small samples (on the order of one gram) was indeed viable. Because of the expense and difficulty of optimizing TIGR from plutonium dioxide, TIGR

optimization tests using ceria have continued. This document details the relationship between the ceria surrogate tests and those conducted using plutonia.

Experimental Procedure

Sample Preparation

The MOX ceria surrogate is composed of CeO_2 that is initially doped with approximately 2 wt% Ga_2O_3 . Fabrication of the surrogates is reported in detail in previous publications.^{1,2} The mixture of cerium and gallium oxide powders is vibration milled for 15-20 min. The powder is then pressed as a green pellet to 30-40% of theoretical density. The resulting pellet is again milled and sifted through a -150 μm screen and pressed into a green pellet (60-70% of theoretical density). The pellet (0.6-0.7 cm O.D. and 1.0-1.2 cm height) is then fired at 450°C for 4 hrs to remove the binder, subsequently heat treated at 1650°C for 4 hrs in air (heating rate of 10°C/min), then followed by a furnace cool. Sintering results in a loss of roughly 50% of the starting Ga_2O_3 . The sintered pellet is re-crushed into powder and sieved through a -150 μm screen. Gallium concentrations vary from lot to lot. The gallium concentrations of all lots were measured using a variety of techniques. An alternate method for production of the surrogate powders involves production of Ce-Ga alloy which is subsequently converted to powder via a three step process similar to that used for plutonium or via direct oxidation. Because it results in much more efficient production of sample material, this technique will be used for producing powder for the full scale cold prototype testing of the TIGR system.

Weapons grade plutonium was converted to oxide using a three-step process: metal to hydride, hydride to nitride, and finally nitride to oxide. The particle size distribution is bimodal with particle size peaks at 1 μm and 40 μm . The powder contains 8700 wppm gallium (0.87wt%).

Figure 1 compares the gallium concentrations of the ceria (7800 wppm) and plutonia powders prior to TIGR. Although the starting Ga_2O_3 concentrations of the plutonia and ceria surrogate materials are similar in weight percent, the atomic percents are less comparable (1.1 at% in plutonia, 0.64 at% in ceria).

Test Procedure

TIGR tests for ceria and plutonia samples incorporated Ar - 6 % H_2 flow velocities of 1.5, 3.0, and 6.0 cm/s, test temperatures of 600-1200°C, test durations (at temperature) of 0.5 to 4 hrs,

and sample sizes of 0.3, 0.9, and 2.5g. Powders were placed into inert alumina crucibles. After exposure, the samples were cooled to room temperature in Ar - 6 % H₂. Weights and gallium concentrations were documented before and after exposure. Gallium concentrations were analyzed by a variety of methods for ceria samples. Plutonia samples were analyzed using inductively coupled plasma - mass spectroscopy.

Results and Discussion

Comparison of TIGR from Ceria and Plutonia

Figure 2 shows the microstructure of a sintered surrogate pellet. The micrograph shows agglomerated grains and pores during sintering. The x-ray elemental map on the bottom associated with the SEM image shows strong gallium intensities at grain boundaries. The gallium-rich regions at the grain boundaries are still observed after exposing this solid pellet to Ar - 6 % H₂ at 1200°C for 4 hrs.¹ This was the first indication that a phase might form under reducing conditions in the CeO₂ (PuO₂)-Ga₂O₃ system from which Ga₂O might volatilize more slowly than from pure Ga₂O₃. Although this phase is not clearly observed in the surrogate TIGR tests (which are performed on powdered material) it is still thought to play a role in the rate of Ga removal.

TIGR tests using pure Ga₂O₃ powder exposed to Ar-6%H₂ at 1200°C for 30 min were performed (Figure 3). The plot shows that relatively large weight losses from 2.5 g samples of Ga₂O₃ occurred (0.6 to 0.9 g) and that weight loss is dependent on flow rate. These losses are much larger than the Ga₂O₃ losses in the surrogate (0.04 g). The gallium concentration change during sintering (Figure 1), morphology (Figure 2), and the amount of vaporization of Ga₂O₃ (Figure 3) show that during sintering, Ga₂O vaporizes from the powder. Under reducing conditions, the remaining Ga₂O₃ is hypothesized to react with CeO₂ to form the CeGaO₃ perovskite phase (discussed below) due to low solubility of gallium in CeO₂.² The fact that this phase has been observed after sintering in a reducing environment suggests that it reduces more slowly than Ga₂O₃ and therefore may control the rate at which the last few percent of Ga initially present is removed. Because the gallium solubility in ceria and plutonia is similar,^{3,4} gallium segregation in the plutonia should be similar. Thus it is possible that TIGR optimization may depend on the extent of formation of this ternary compound.

The possible vaporization species from gallium oxides are reported in the literature as Ga₂O, GaO, GaOH, and metallic gallium during thermal vaporization.^{3,5} Thermodynamic calculations of the Ga-O-H system and x-ray photon electron spectroscopy studies of the

deposition product indicated that during high-temperature exposure of Ga_2O_3 to H_2 , Ga_2O_3 will vaporize as predominantly $\text{Ga}_2\text{O}(\text{g})$.¹ As the gas product is transported to cooler regions of the furnace, the $\text{Ga}_2\text{O}(\text{g})$ will back react with $\text{H}_2(\text{g})$ and $\text{H}_2\text{O}(\text{g})$ and will condense out as $\text{Ga}(\text{l})$ and Ga_2O_3 .¹ Thus, understanding the behavior of Ga_2O vaporization is critical to optimizing TIGR from plutonia.

The weight change results of both ceria surrogate and plutonia exposed to Ar-6% H_2 for 30 minutes of exposure are shown as a function of sample size in Figure 4. Each bar in Figure 4 represents an average value. The effect of lot size is stronger in the plutonia, where increasing lot size results in decreasing weight loss. Both ceria and plutonia show increasing weight loss with increasing temperature. The weight loss is attributable to the mass loss associated with gallium evolution and plutonia or ceria reduction.^{1,5,7,8} Therefore weight loss alone is only a semi-quantitative measure of gallium loss.

Figure 5 compares the TIGR behavior of ceria and plutonia as a function of temperature, as measured by weight loss. Not only do the ceria and plutonia weight losses vary similarly as a function of temperature, but the absolute values of weight loss are comparable. This suggests that ceria is an excellent surrogate for plutonia with respect to TIGR. Figures 4 and 5 verify that weight loss due to TIGR is strongly affected by temperature. Temperatures of at least 1000°C are required for significant TIGR.^{1,2,6} There is some correlation between weight loss and remaining gallium concentration (Figure 6) for both ceria and plutonia. While similar in form, these relationships are different due to differences in both gallium loss and (particularly) the amount of oxide (ceria or plutonia) reduction.

Figure 7 is a comparison of tests incorporating low gas flow velocity (1.5 cm/s) and those incorporating higher flow velocities (3.0 and 6.0 cm/s) following TIGR of ceria and plutonia. Data are from tests incorporating various temperatures (600-1200°C), lot sizes (0.3, 0.9, 2.5g powder), and test durations (0.5 h and 4 h). There is no discernible effect of flow rate on TIGR efficiency. This implies that the rate controlling mechanisms for both ceria and plutonia may be identical. It also does not negate the hypothesis that the rate limiting step for TIGR may be solid state diffusion at 1200°C because there is a flow rate effect on reduction of pure Ga_2O_3 (Figure 3).⁶ However, at this time, there is insufficient data to support an argument for any particular rate controlling mechanism.

Comparison of Thermodynamic Properties of Ceria and Plutonia

The molar heat capacities of many substances can be calculated using the following equation:⁹

$$C_p(T) = A + BT + CT^2 + DT^{-2} \quad (2)$$

where A, B, C, D are constants and T is the temperature (K). If the value of the enthalpy at room temperature is known ($H_{298.15}$), then the enthalpy at any temperature can be calculated using:

$$H(T) = H_{298.15} + \int_{298.15}^{T_1} C_{p1}(\tau) d\tau + \Delta H_{T_1} + \int_{T_1}^T C_{p2}(\tau) d\tau \quad (3)$$

where T_1 is the temperature of a phase transformation (if any). Additional terms describing other phase transformations can be included.

The entropy is also related to the heat capacity and, if the value of the entropy at room temperature is known, then the entropy at higher temperatures can be calculated via

$$S(T) = S_{298.15} + \int_{298.15}^{T_1} \frac{C_{p1}(\tau)}{\tau} d\tau + \frac{\Delta H_{T_1}}{T_1} + \int_{T_1}^T \frac{C_{p2}(\tau)}{\tau} d\tau \quad (4)$$

The Gibbs free energy can now be calculated since equation 4 provides a relationship involving the enthalpy and the entropy that are already known.

$$G(T) = H(T) - T \cdot S(T) \quad (5)$$

Substituting equation 2 into equations 3-5, the following expression for the Gibbs free energy is obtained:

$$G(T) = G_1 + G_2 T - AT \ln T - B \frac{T^2}{2} - C \frac{T^3}{6} - D \frac{T^{-1}}{2} \quad (6)$$

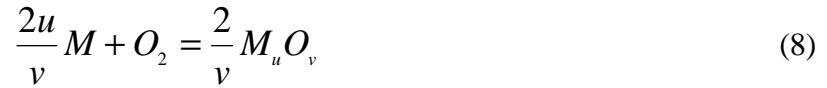
where G_1 and G_2 are integration constants, related to $H_{298.15}$ and $S_{298.15}$.

Since the heat capacity of most liquids is a constant with respect to the temperature, the Gibbs free energy of the liquid phase can be described using equation 7:

$$G_l(T) = G_{1l} + G_{2l} T - A_l T \ln T \quad (7)$$

Information about the thermodynamic properties of plutonium oxide and cerium oxide systems for these calculations was extracted from the literature.⁹⁻¹² The regression of the experimental data leads to a set of coefficients that can be used in the description of all of the thermodynamic functions discussed above. For the purpose of this work, only the results for the Gibbs free energy are shown in Figure 8 for several plutonium and cerium oxides. One can notice the similarity between the values for PuO_2 and CeO_2 and also between the values for the sesquioxides.

Figure 9 shows the values of the Gibbs free energy of formation, calculated for the following reaction:



where u and v are arbitrary numbers and equation 8 involves only one mole of oxygen. This Ellingham-Richardson type diagram is widely used for comparing the stability of different oxides. One can notice a similarity between the two groups of oxides; PuO_2 - CeO_2 and Pu_2O_3 - Ce_2O_3 . The similarities in Gibbs energies (Figures 8 and 9) suggests that there is a fundamental basis for similarities in TIGR from ceria and plutonia.

The Ga rich phase discussed above is thought to be a perovskite phase $Ce(or Pu)GaO_3$. The thermodynamic comparison is included here to support the conclusion that this phase is likely to contribute to the final rate controlling step and thereby the residual Ga level under a particular set of conditions in both systems.

CeGaO₃ Stability

Leonov et al¹⁴ have tried to synthesize $CeGaO_3$ from molar ratios of Ce_2O_3/Ga_2O_3 equal to 1:1, 3:5, and 1:11. The synthesis was conducted in oxidizing and inert gas environments at temperatures from 1273 K to 1973K. No chemical compounds of defined structure or solid solutions were formed.

When the synthesis was conducted in H_2 or NH_3 at 1273 K, $CeGaO_3$ formed. However, completeness of the reaction was not achieved even in the case of repeated heating with intermediate grinding. Synthesis at 1573 K, 1673 K, and 1773 K indicated that gallium oxide is intensively volatilized. They were able to synthesize $CeGaO_3$ in an evacuated and sealed quartz tube at 1573 K by the reaction:



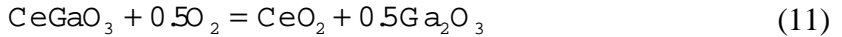
Examination of isothermal $\Delta G(O_2)$ change with composition for the Ce-O and Ga-O binaries suggest that $CeGaO_3$ undergoes a reducing disproportionation by the reaction



at $\log(P_{O_2}) = -12.77$. Solving the ΔG_{rxn} equation yields $\Delta G_{f<CeGaO_3>}$ equal to -96.3 kJ/mole.

Further examination of $\Delta G(O_2)$ change with composition suggest that $CeGaO_3$ undergoes an

oxidizing disproportionation by the reaction



Using the value for $\Delta G_f^{\circ}(\text{CeGaO}_3)$ yields a $\log(\text{PO}_2)$ value equal -4.91. The results are shown in Figure 10.

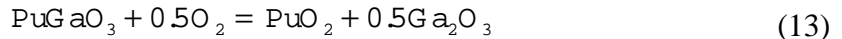
PuGaO₃ Stability

Examination of isothermal $\Delta G(\text{O}_2)$ change with composition for the Pu-O and Ga-O binaries suggest that PuGaO_3 undergoes a reducing disproportionation at 1500 K by the reaction:



at $\log(\text{PO}_2) = -13.93$. Solving the ΔG_{rxn} equation yields $\Delta G_f^{\circ}(\text{PuGaO}_3)$ equal to -96.6 kJ/mole.

Further examination of $\Delta G(\text{O}_2)$ change with composition suggests that PuGaO_3 undergoes an oxidizing disproportionation by the reaction



Using the value for $\Delta G_f^{\circ}(\text{PuGaO}_3)$ yields $\log(\text{PO}_2) = -6.89$. The results are shown in Figure 11.

Based on the dependency of the partial pressure of oxygen upon the temperature, at thermodynamic equilibrium, the limits of stability for the Pu(Ce)O₃ perovskites can be calculated. The stability diagram (Figure 12) shows how similar the limits are for both PuGaO_3 and CeGaO_3 . This is one more argument supporting the use of cerium oxides as surrogates for the plutonium oxides.

One can note that the perovskite structures can not be obtained (at reasonable temperatures) in normal conditions of atmospheric oxygen pressure (in air). If the partial pressure of oxygen is 10^{-10} , then both compounds are stable between 715 K and 1250 K. For a partial pressure of oxygen of 10^{-20} , the stability limits are 1100-1825 K for CeGaO_3 and 1175-1825 K for PuGaO_3 . So the likelihood of generating the perovskites is proportional to the severity of the reducing atmosphere.

Conclusions

A detailed study of TIGR from ceria was undertaken. These tests provide a basis for the understanding of TIGR without the use of radioactive materials thereby saving money and time, and reducing worker exposure. Surrogate tests revealed microstructural information that is difficult to obtain with plutonia. A comparison of ceria and plutonia data suggests that the gallia-doped ceria is a good surrogate for plutonia. Weight loss data from the plutonia and ceria suggest that temperature has a stronger influence on TIGR than other variables examined (flow rate, lot size, test duration). The similarity in thermodynamic properties of ceria and plutonia suggests that there is a fundamental basis for the empirical observations. It is concluded that the ceria surrogate tests, which can be performed more cheaply and readily, provide an insight into TIGR from plutonia that is very difficult to obtain using plutonia itself.

References

1. D. P. Butt, Y. S. Park, and T. Taylor, "Thermal Vaporization and Deposition of Gallium Oxide in Hydrogen", *J. of Nucl. Mater.*, **264**, 71 (1999).
2. Y. S. Park and D. P. Butt, "Kinetics and Atmospheric Effects on Gallium Removal from a CeO₂ Based Mixed Oxide Surrogate", Proceedings of the 100th American Ceramic Society Conference, 1998.
3. D. R. Lide, Handbook of Chemistry and Physics, 77th Edition, (1996-1997).
4. C. Guminski, "Solubility of Metals in Liquid Low-Melting Metals", *Z. Metallkd.*, **81**, 105 (1990).
5. G. V. Samsonov, The Oxide Handbook, IFI/Plenum Data Corporation, 1973.
6. Y. S. Park and D. P. Butt, "Thermally Induced Gallium Removal from a CeO_{2-x} as a PuO_{2-x} Surrogate", to be submitted to *J. of Nucl. Mater.*, 1999.
7. A. Laachir, V. Perrichon, A. Badri, J. Lamontte, E. Catherine, J. C. Lavalley, J. E. Fallah, L. Hilaire, F. I. Normand, G. N. Sauvion, and O. Touret, "Reduction of CeO₂ by Hydrogen," *J. Chem. Soc. Faraday Trans.*, **87**, 1601 (1991).
8. M. Romeo, K. Bak, J. E. Fallah, F. L. Normand, and L. Hilaire, "XPS Study of the Reduction of Cerium Dioxide", *Surface and Interface Analysis*, **20**, 508 (1993).
9. O. Kubaschewski, C. B. Alcock, "Metallurgical Thermochemistry", Pergamon Press, London, 1979.
10. L. B. Pankratz, "Thermodynamic properties of elements and oxides", U.S. Bureau Of Mines Bulletin 672, Supt. Of Docs., Washington, D.C., 1982.
11. L. B. Pankratz, "Thermodynamic properties of halides", U.S. Bureau Of Mines Bulletin 674, Supt. Of Docs., Washington, D.C., 1984.

12. D. D. Wagan, W.H. Evans, V.B. Parker, R.H. Schumm, I. Halow, S.M. Bailey, K. L. Churney, and R. L. Nuttal, "The NBS tables of chemical thermodynamic properties", National Bureau of Standards, Washington, D.C., 1982.
13. S. L. Eaton, R. Hanrahan, D. P. Butt, M. Stan, C. Haertling, Y. Park, "Nuclear Fuels Technologies Fiscal Year 1998 Fuel Fabrication Development Ga Sintering Summary Report", LANL report LA-UR-98-4932, 1998.
14. A. I. Leonov, A. V. Andreeva, V. E. Shvaiko-Shvaikovskii, and E. K. temperature chemistry of cerium in the systems cerium oxides- Al_2O_3 , Cr_2C Neorganicheskie Materialy, 2, 517 (1966).

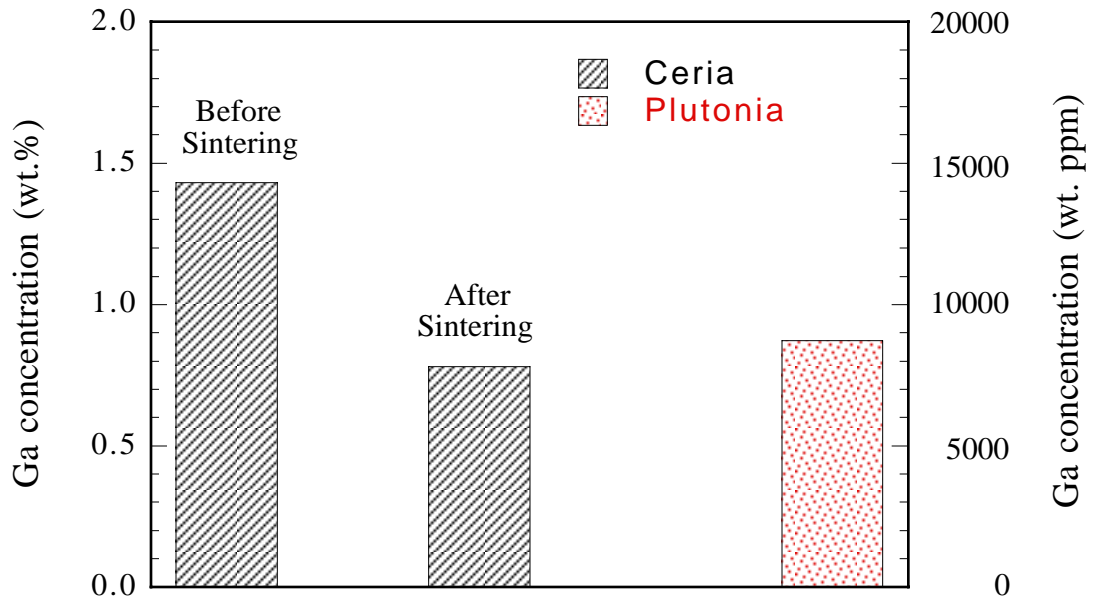


Figure 1. Gallium concentration in ceria surrogate powders before and after sintering compared to three-step plutonia powder.

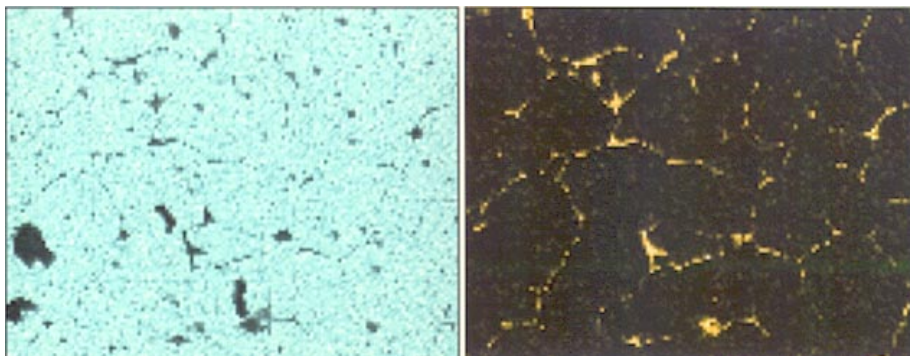
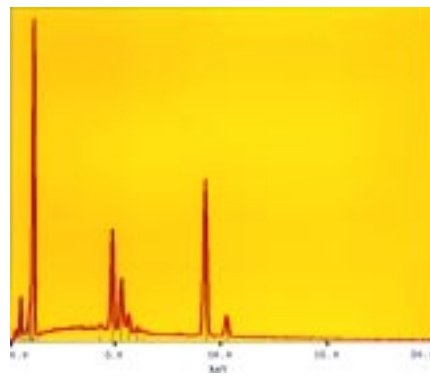
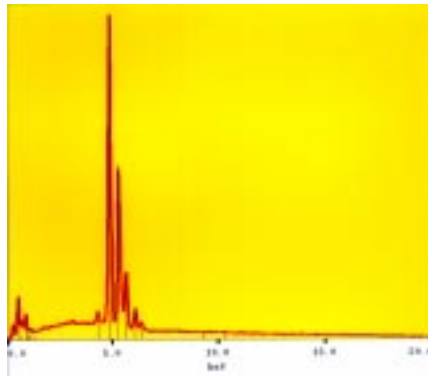
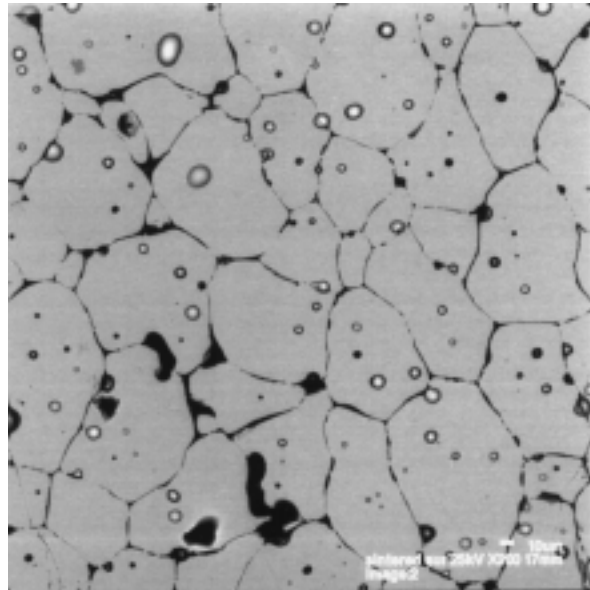


Figure 2. Top: SEM image of the cross section of a sintered ceria pellet. Middle left: EDS pattern from CeO₂ matrix. Middle right: Gallium rich area in the grain boundary . Bottom: X-ray maps show cerium (left) and gallium (right) intensities.

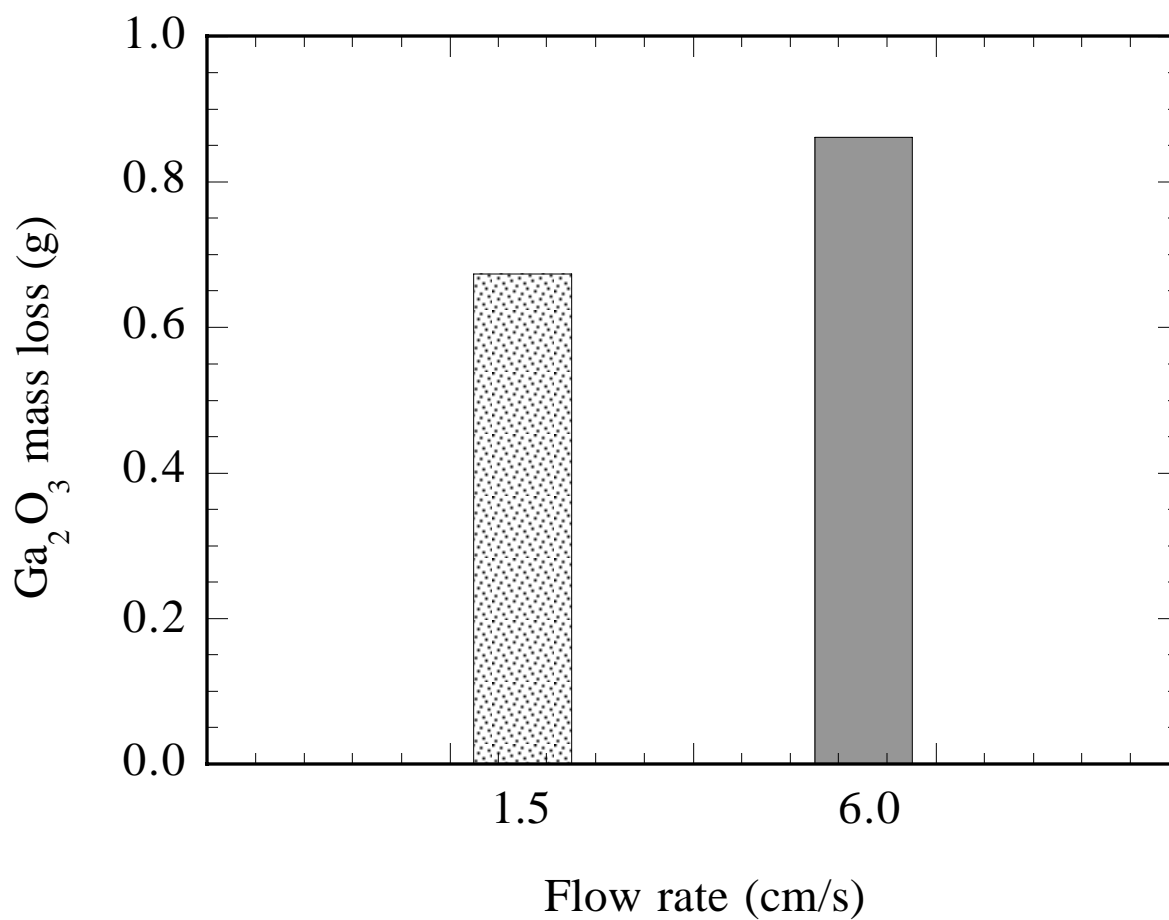


Figure 3. Mass loss from 2.5 g samples of Ga₂O₃ powder exposed to Ar-6%H₂ at 1200°C for 30 min.

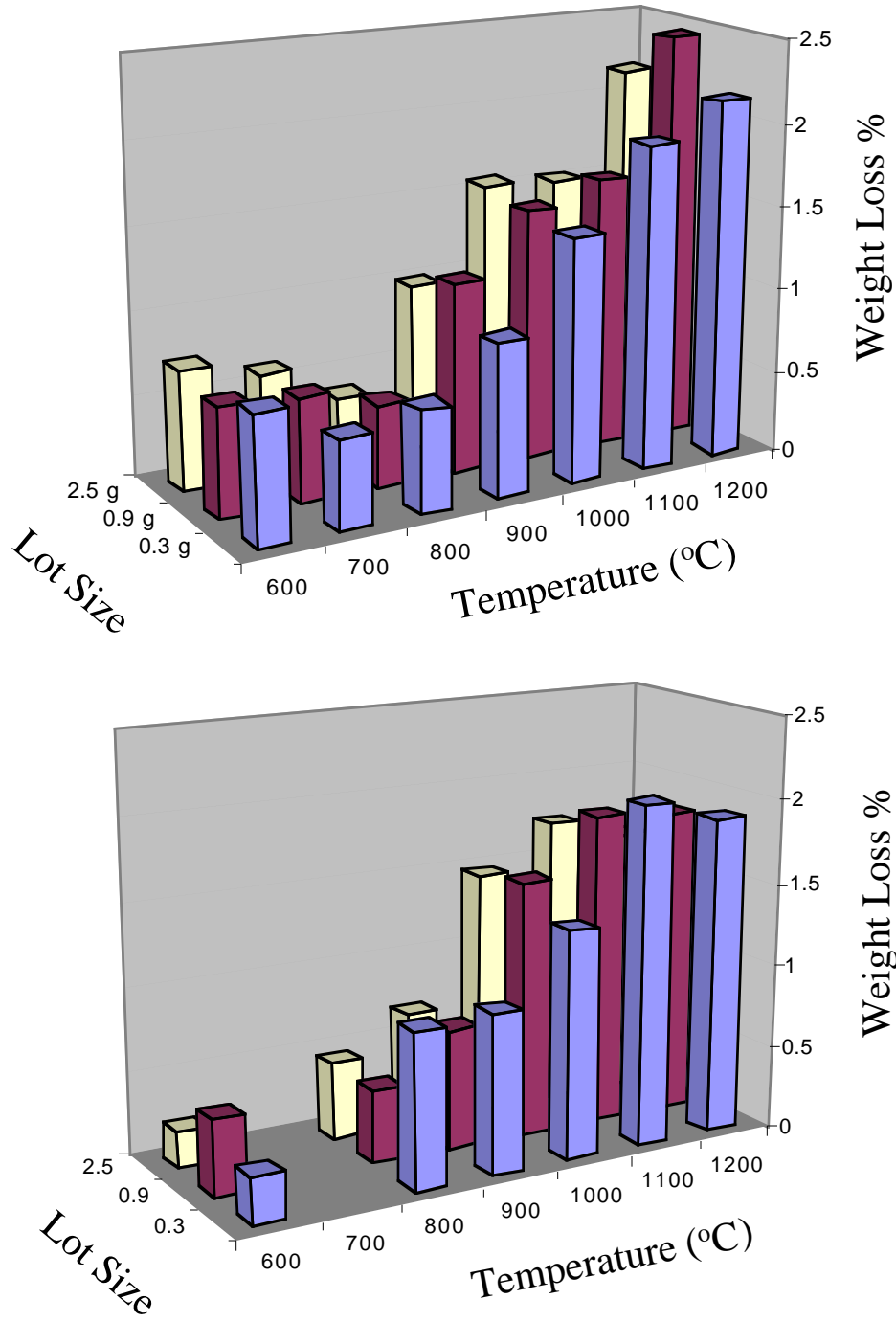


Figure 4. Weight loss comparison between ceria (above) and plutonia (below) exposed to Ar-6% H₂ for 30 min. at a flow rate 1.5 cm/sec.

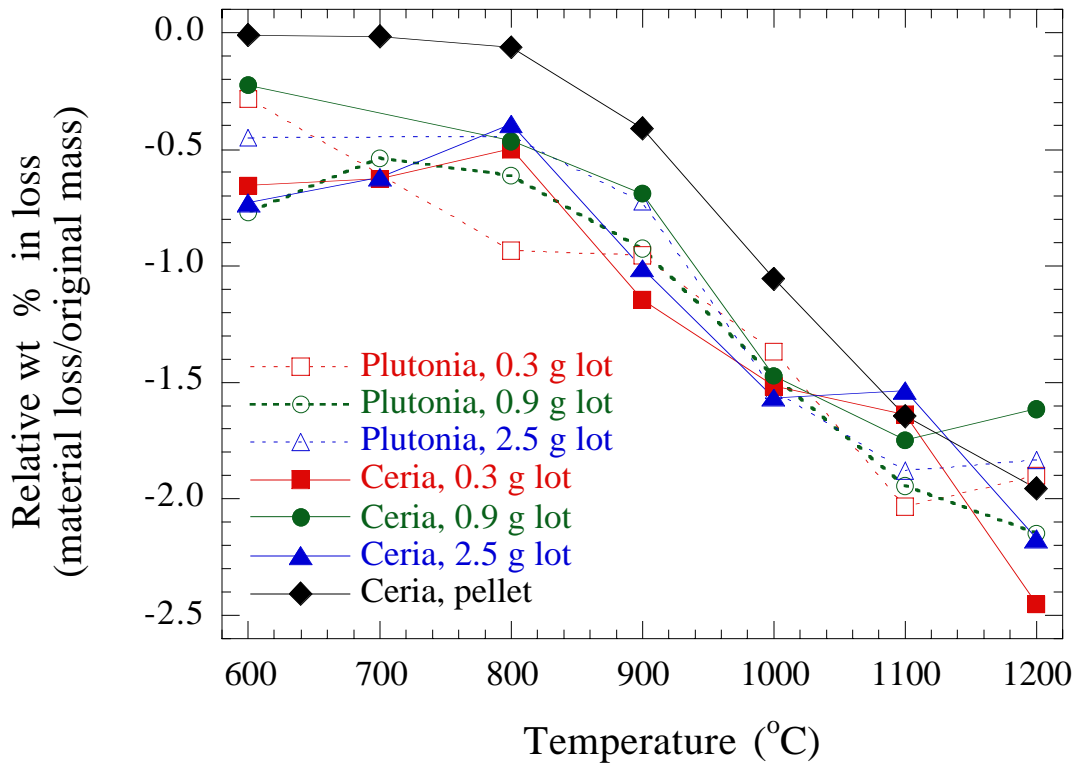


Figure 5. Weight loss from ceria and plutonia exposed to Ar-6% H_2 for 0.5 h as a function of temperature and lot size.

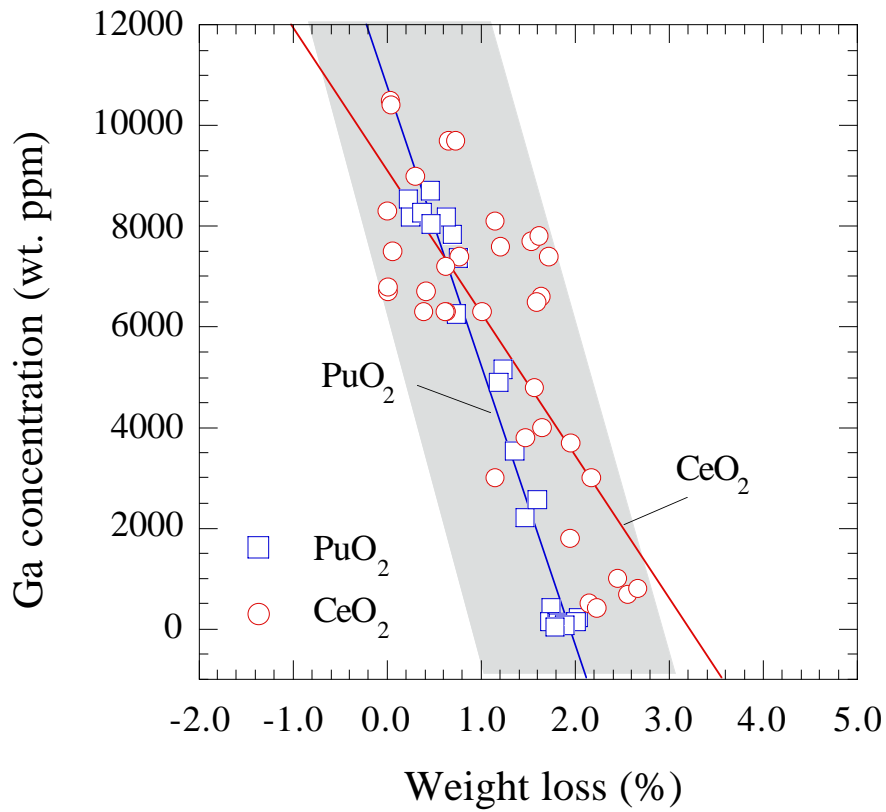


Figure 6. Comparison of gallium concentration remaining in the material as a function of weight loss for both ceria and plutonia. Tests incorporate a variety of temperatures (600°C to 1200°C), durations (0.5 to 4 hrs), flow rates (1.5 to 3.0 cm/sec), and lot sizes (0.3, 0.9, 2.5 g powder and pellet).

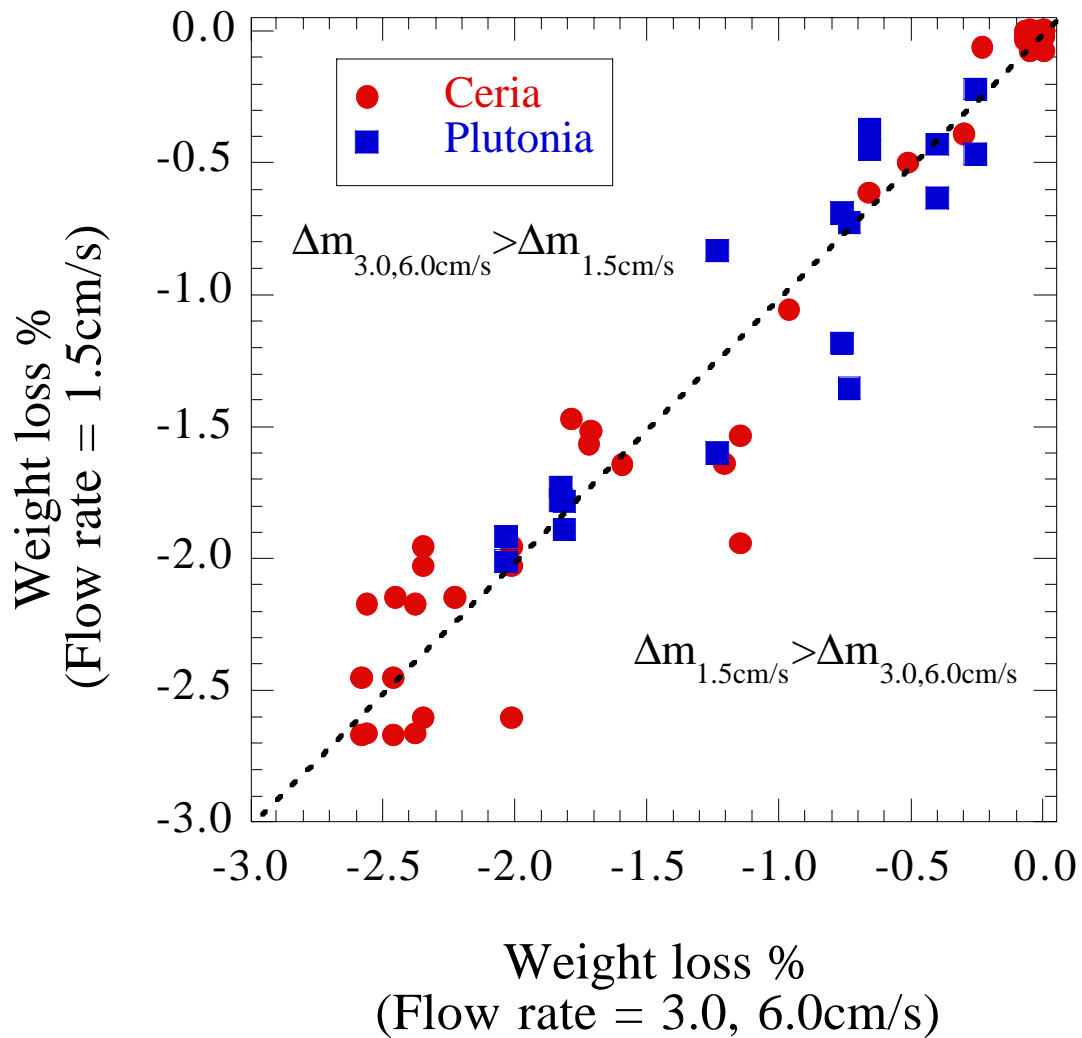


Figure 7. A comparison of weight loss at low flow velocities (1.5 cm/s) to those at higher flow velocities. Both ceria and plutonia data are derived from tests incorporating various temperatures and lot sizes, and test durations of 0.5 h.

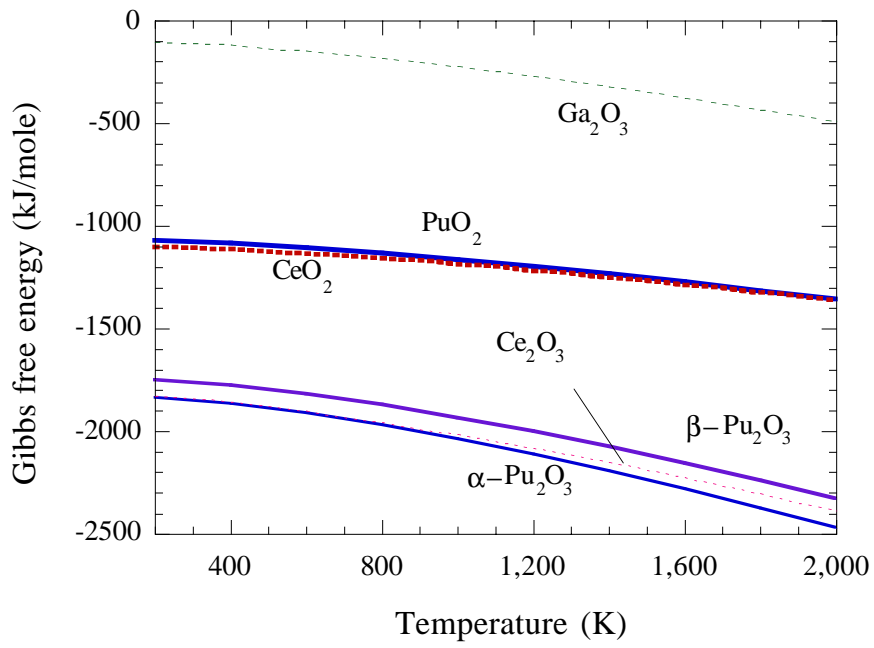


Figure 8. The Gibbs free energy of several plutonium and cerium oxides systems.

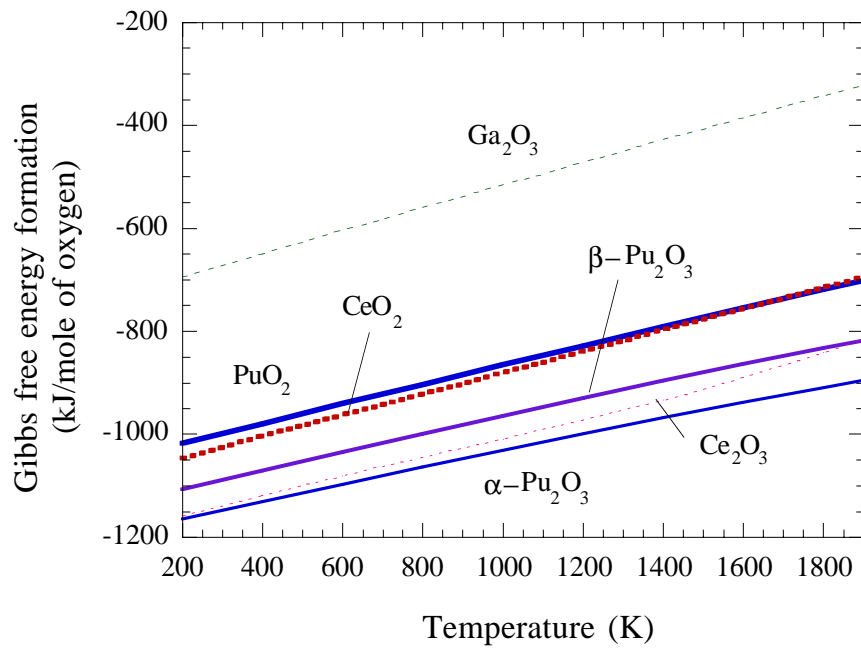


Figure 9. The Gibbs free energy of formation of several plutonium and cerium oxides, when only one mole of oxygen is involved (Ellingham diagram).

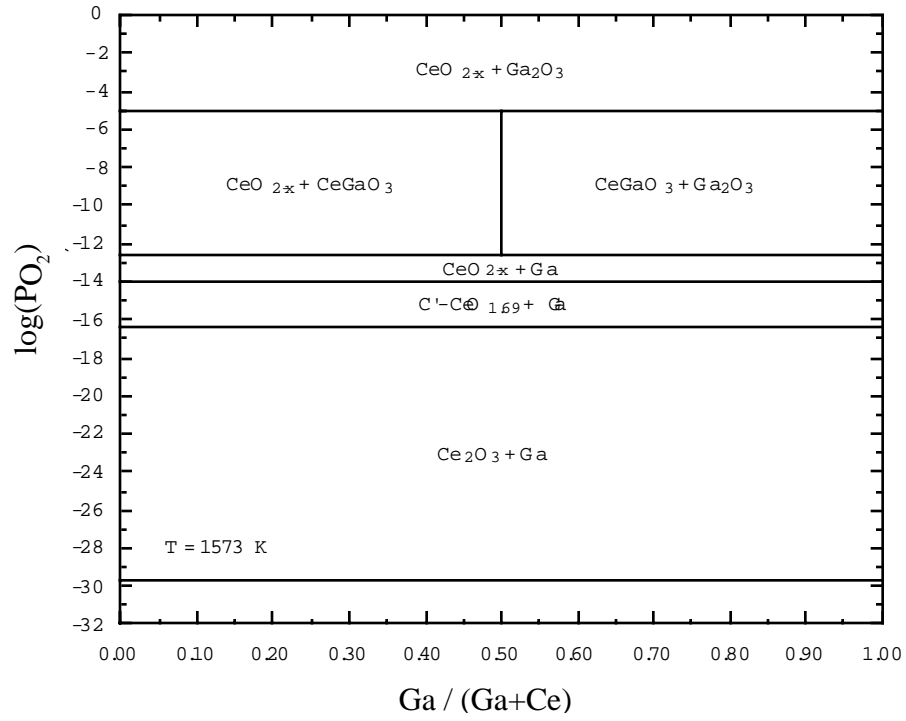


Figure 10. Equilibrium phase diagram of $\log P_{O_2} = f\left(\frac{Ga}{Ce+Ga}\right)$ for the Ce-Ga-O system at 1573 K.

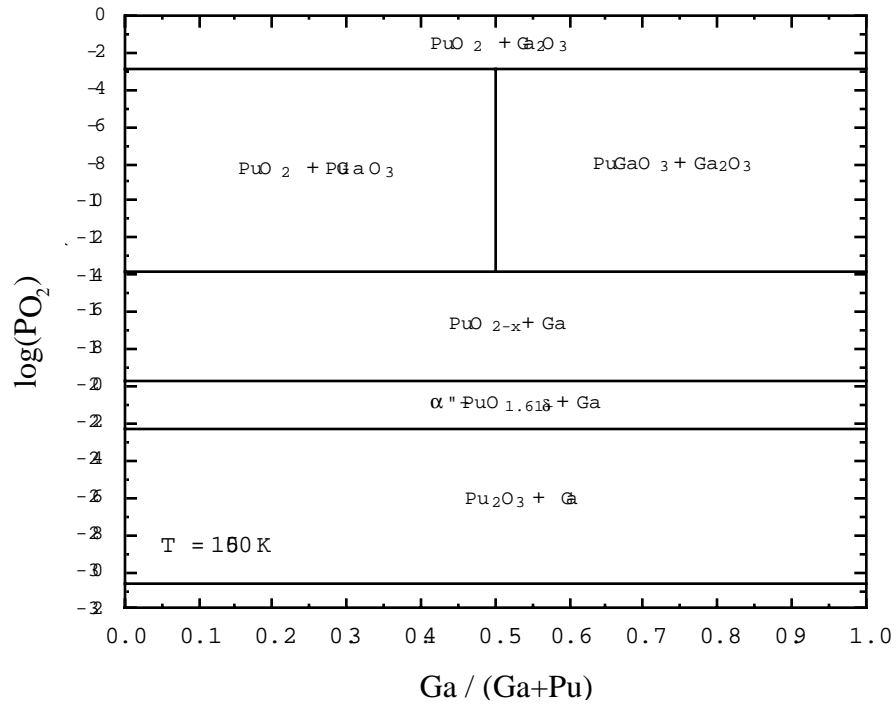


Figure 11. Equilibrium phase diagram of $\log P_{O_2} = f\left(\frac{Ga}{Pu+Ga}\right)$ for the Pu-Ga system at 1500 K.

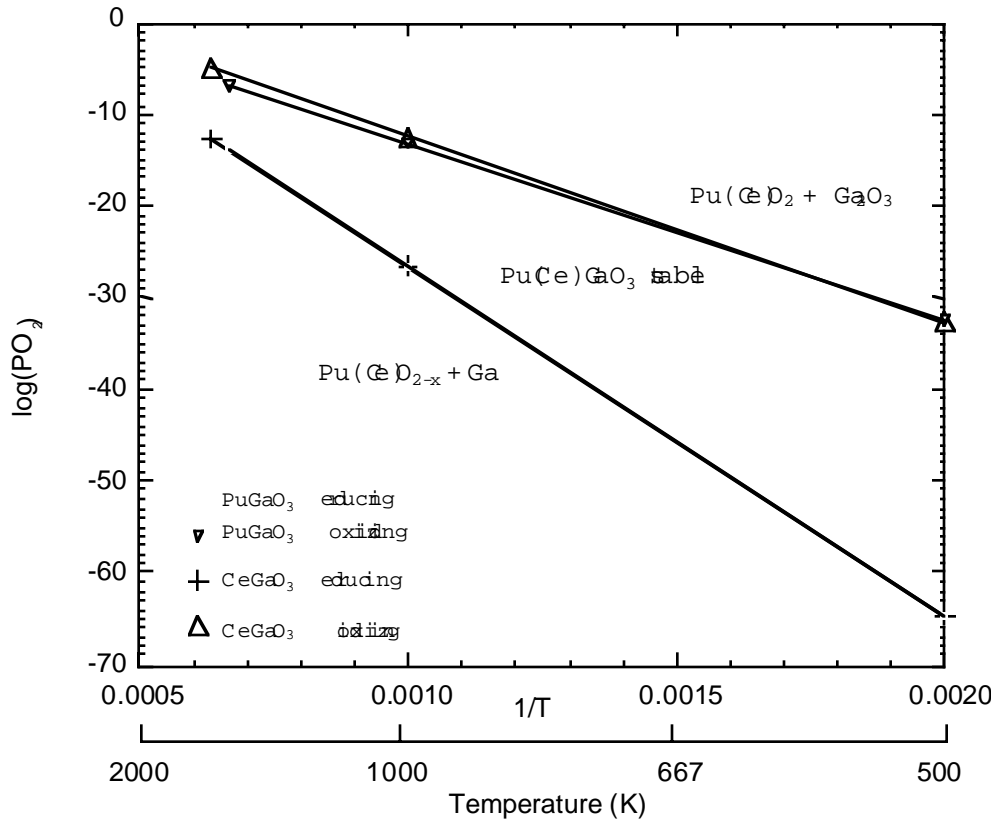


Figure 12. Diagram of $\log (P_{O_2}) = f(1/T)$ defining PuGaO_3 and CeGaO_3 zones of stability.